LA-UR-19-26783 (Accepted Manuscript)

Correction of Factor Effects for Simultaneous Collection of Elemental Analysis and Relaxation Times by Nuclear Magnetic Resonance

Widgeon Paisner, Scarlett
Janicke, Michael Timothy
Kaseman, Derrick
Yoder, Jacob Luther
Alvarez, Marc Anthony
Espy, Michelle A.
Williams, Robert F.

To be published in: Analytical Chemistry

DOI to publisher's version: 10.1021/acs.analchem.9b05603

Permalink to record: http://permalink.lanl.gov/object/view?what=info:lanl-repo/lareport/LA-UR-19-26783

Correction of *Q* factor effects for simultaneous collection of elemental analysis and relaxation times by nuclear magnetic resonance

Scarlett Widgeon Paisner[1*], Michael T. Janicke[2], Derrick C. Kaseman[3], Rachel K. Frankle[3], Jacob L. Yoder[3], Marc A. Alvarez[3], Michelle A. Espy[4], Robert F. Williams[3]

[1]Materials Science in Radiation and Dynamics Extremes, Los Alamos National Laboratory, Los Alamos, NM USA

[2]Inorganic, Isotope and Actinide Chemistry, Los Alamos National Laboratory, Los Alamos, NM USA

[3]Bioenergy and Biome Sciences, Los Alamos National Laboratory, Los Alamos, NM USA

[4]Non-destructive Testing and Evaluation, Los Alamos National Laboratory, Los Alamos, NM USA

ABSTRACT: A new method for measurement of elemental analysis by nuclear magnetic resonance (NMR) of unknown samples has been discussed here as a quick and robust means to measure elemental ratios without the use of internal or external calibration standards. The determination of elemental ratios was done by normalizing the signal intensities by the frequency dependent quality factor (Q) and the gyromagnetic ratios (γ) for each measured nucleus. The correction for the frequency dependence was found by characterizing the output signal of the probe as a function of the quality factor (Q) and the frequency, and the correction for γ was discussed in a previous study. A Carr-Purcell-Meiboom-Gill (CPMG) pulse sequence was used for evaluation of the relative signal intensities and allows for derivation of elemental ratios, and was correspondingly used to simultaneously measure the T_2^* of samples for an added parameter for more accurate identification of unknown samples.

INTRODUCTION Quantitative analysis by nuclear magnetic resonance (NMR) has been used extensively in pharmaceutical, medical, and analytical chemistry due to the non-destructive nature and a low detection limit of parts per billion.[1–4] In particular, NMR has been used to determine the purity of pharmaceuticals and organic solutions and can detect relative ratios of different stereoisomers, constitutional isomers, and enantiomers in solution.[5–7] In order to acquire quantitative data, calibration standards and methods are employed. These include external or internal standards and the Electronic Reference To access In vivo Concentration (ERETIC) method.[8] Addition of an internal calibration standard requires a known quantity of a standard to be added to the sample, which is then compared to the signal area of the unknown substance. This requires some knowledge unknown sample chemistry, since the internal standard must be a substance that is inert in the solution. The external calibration standard requires generation of a calibration curve and is most accurate when concentrations of the standard are close to the concentration of the unknown sample. This method also necessitates approximate knowledge of the sample concentration and chemistry to create an accurate calibration curve. The ERETIC method utilizes an electrical reference signal that is implemented when collecting the spectra of unknown samples, and this electrical signal is calibrated against a standard of known concentration. When elemental analysis of several nuclei are desired, the process to determine the elemental ratios of a sample is time consuming for the three aforementioned methods since each nucleus must be calibrated independently, which is time consuming and inefficient. This makes NMR less desirable as a quantitative tool in the aforementioned industries, and therefore other analytical tools are more readily applied.

However, for rapid analysis where relative ratios of various elements are sufficient for identification of an unknown sample instead of absolute concentrations, it is possible to measure the ratios without the use of any external or internal standards. Takeda and colleagues[9] have shown this previously by correcting for differences in the gyromagnetic ratio, γ. This was accomplished by sweeping the magnetic field and holding the frequency constant for each nucleus. The sensitivity of each nucleus depends on γ and this causes unequal contributions of signal for each isotope; therefore, differences in γ restrict and prevent direct comparisons. The effect of different γ values for different nuclei can be corrected by applying the receptivity coefficient for constant frequency (D_{cf}), and is determined to be:

$$D_{cf} = x_k|\gamma_k|I_k(I_k + 1) \quad (1)$$

where x_k represents the natural abundance and I_k is the spin quantum number of nucleus k. Equation (1) demonstrates a constant frequency measurement, in which the magnetic field is varied to measure each nucleus. By applying D_{cf}, Takeda and colleagues were able to determine the relative fraction of H, P, and Na atoms in a NaH_2PO_4 solution with an error of less than 4%. This is possible since at constant frequency the efficiency of the electrical circuit of the probe and the quality factor (Q) remain unchanged.

A constant frequency experiment requires a variable field magnet which makes this approach unfeasible for conventional, fixed field NMR. When carrying out a fixed magnetic field experiment, the resonant frequency is different for each nucleus. This is more common compared to constant frequency measurements due to the availability of high magnetic field superconducting magnets. In this case, the receptivity equation is modified by incorporating a cubed dependence of γ_k. This is referred to as the receptivity for constant magnetic field (D_{cB}) as is shown in Equation (2):[9]

$$D_{cB} = x_k|\gamma_k|^3 I_k(I_k + 1). \quad (2)$$

The cubed factor of γ_k is a result of a squared dependence from the thermal magnetization as defined by Curie's Law and another factor of γ_k from the Larmor frequency, ω_o, of each nucleus.[10] Although this equation does address the issue of different γ for the various isotopes, it does not account for the frequency dependence of the signal from the resonant circuitry electronics. The frequency dependence of Q is a measure of the efficiency of an electrical circuit and is defined as a resonator's bandwidth with respect to the central frequency, as is shown in Equation (3):

$$Q = {}^{\omega_0 L}/_{R} \quad (3)$$

where R is an effective resistance that accounts for the resistive losses of the circuit and dielectric/resistive losses of the sample, and L is the inductance of the coil. Note that in the constant frequency case illustrated above, Q will be constant. Q can be measured with a network analyzer using the observed frequency divided by the bandwidth. For a single probe configuration, Q is then dependent on the dielectric and resistive losses of the sample, the coil resistance, and the frequency, where the former can be related to the polarity of the sample. Q is related to the signal:noise ratio (SNR) (ψ) as described by Equation (4):[10–12]

$$\Psi = K\eta M_0 \left({}^{\mu_0 Q \omega_0 V_c}/_{4Fk_B T_c \Delta f}\right)^{0.5}. \quad (4)$$

K describes the geometry of the receiving coil and is typically close to 1, η is the fill factor of the coil, M_o is the nuclear magnetization, μ_o is the permeability of free space, V_c is the volume of the coil, F describes the inherent noise of the preamplifier, k_B is the Boltzmann constant, T_c is the temperature of the coil, and Δf is the receiver bandwidth. k_B and μ_o are constants, and for a singular probe configuration, K, V_c, F, T_c, and Δf are also constant and they all can be combined into the term, A. With carefully prepared samples in NMR tubes with constant volume, η can also be considered as a constant and be included in A. The nuclear magnetization in thermal equilibrium, M_o, is defined as

$$M_0 = \frac{N\gamma h^2 I(I+1)\omega_0}{4\pi^2 k T_s}$$

where N is the number of nuclei, h is Plank's constant, k is the Boltzmann constant, and T_s is the sample temperature. Clearly M_o is proportional to the frequency, ω_o, and can be substituted in Equation (4) while the other terms are constant (assuming 100% natural abundance) and can be grouped into term C.[10] If the noise is constant for a specific probe and console configuration, it can also be incorporated into A so that frequency and Q can be directly related to signal intensity (S). By applying these substitutions and A to Equation (4), the following relation is derived:

$$S \approx C\omega_0^{1.5} Q^{0.5}. \quad (5)$$

The signal intensity is then simply related to only two easily measured parameters Q and ω_o. From this equation, the signal response of nuclei at different frequencies can be related.

Elemental analysis is an important parameter for the identification of unknowns, but in some cases, it can be misleading if only naturally abundant NMR nuclei are measured. Such examples are dichloroethane ($C_2H_4Cl_2$) and acetaldehyde ($C_2H_4O_2$), which have the same C:H ratio of 2:4 but also contain other low γ, quadrupolar nuclei that are difficult to measure directly. Here, the accuracy of distinguishing between the molecules could benefit from considering another signature to differentiate the two, such as the transverse relaxation time (T_2). T_2 is dependent on paramagnetic impurities in the sample, the mobility of the molecules in solution, chemical shift anisotropy, chemical exchange, and dipolar coupling.[13] Therefore, the T_2 relaxation processes between different molecules are likely different and the T_2 time constant can be used as an additional dimension in the signature space. However, the measured T_2 value may be shorter than the theoretical T_2 value

caused by molecular diffusion in an inhomogeneous magnetic field. Equation (6) shows the relationship of the measured T_2 value (referred to as T_2^*), which is a sum of the inverse of the inherent T_2 and the additional T_2 contributions that arise from molecular diffusion in an inhomogeneous field (T_{2i}).

$$\frac{1}{T_2^*} = \frac{1}{T_2} + \frac{1}{T_{2i}} \quad (6)$$

The Carr-Purcell-Meiboom-Gill (CPMG) pulse sequence is routinely used to determine T_2^*, and consists of a 90° pulse followed by a train of 180° pulses. Between each 180° pulse, a spin echo forms. The spin echo intensity decreases with each successive 180° pulse, due to T_2^* processes. The intensity decrease follows an exponential decay with time constant T_2^*.[14,15] Although, quantitative NMR measurements are typically carried out using a single-pulse experiment, herein CPMG is also used to collect quantitative information. Quantitation has been previously demonstrated on amino acids and proteins by using the maximum amplitude of the first CPMG echo.[16–18]

In this study, CPMG was used to determine elemental ratios for ^{1}H, ^{19}F, and ^{31}P. We have investigated the impact of varying solvent dielectric constants, different magnetic fields (1 to 3.5 T), and molecular structure on the error of H:F:P elemental ratios. At a field of 3.5 T, these errors are as large as 32%. We demonstrate that these errors may be corrected by measuring Q and normalizing the signal by both Q and D_{cf}. After applying these corrections, elemental ratios with errors of less than 6% are achieved.

EXPERIMENTAL SECTION Bis-(2,2,2 trifluoroethyl)methylphosphonate (BTFEMP) was synthesized by slowly adding 2,2,2-trifluoroethanol (sigma Aldrich) to methylphosphonic dichloride (Sigma-Aldrich) in tetrahydrofuran (THF) (Sigma-Aldrich) at -12 °C. Triethyl amine (Sigma-Aldrich) was then added in excess and the solution stirred overnight. THF was removed by evaporation and the resulting solution was evaluated by thin layer chromatography (TLC). Purification of BTFEMP was accomplished by column chromatography on silica with a mobile phase of 90:10 hexane/ethyl acetate. ^{31}P, ^{13}C, and ^{1}H NMR spectra were collected and show a product purity of >98% for each nuclei. This BTFEMP was used without further purification. A 1M triphenyl phosphate (TPP) (Sigma-Aldrich) solution was prepared using deuterated dimethyl sulfoxide (DMSO) (Cambridge Isoptopes). A 5M diisopropyl methylphosphonate (DIMP) (Alfa Aesar) was prepared in deuterated acetonitrile (Sigma-Aldrich) and isopropyl methyl phosphonate (IMP) (Synquest Laboratories) solution was used neat (without dilution). Trifluoro acetic acid (TFA) (Sigma-Aldrich) was prepared in deuterated water and deuterated acetonitrile (Cambridge Isotopes) at concentrations ranging from 1M to 5M TFA to determine the effect of solvent polarity on our NMR measurements. In order to observe the relationship of Q and frequency, samples of water, acetonitrile (Sigma-Aldrich), toluene (Sigma-Aldrich), and 5M NaCl (Sigma-Aldrich), were also prepared. Precisely 1 mL of the above-mentioned solutions were placed in 5 mm NMR tubes for analysis.

All ^{1}H, ^{19}F, and ^{31}P NMR measurements were collected using a Tecmag Redstone LF2 NMR console with a Cryogenic Ltd. 54 mm bore variable field (0 –7 T) cryogen free magnet. The field has a homogeneity of <20 ppm over a 10 mm diameter spherical volume. The broadband channel of a 5mm Bruker 400 MHZ standard bore probe was used to collect all measurements so that the same coil and electronic circuit were used for each nucleus. For measurements collected at a magnetic field of 1 T for ^{1}H, ^{19}F, and ^{31}P nuclei, the observed frequencies were 42.58, 40.05, and 17.24 MHz, respectively, and measurements collected at 3.5T were observed at frequencies of 149.0, 140.2, and 60.3 MHz, respectively. Constant frequency experiments were collected using a frequency of 42.6 MHz corresponding to magnetic fields of 1, 1.06 and 2.47 T for ^{1}H, ^{19}F, and ^{31}P nuclei, respectively. The Carr-Purcell-Meiboom-Gill (CPMG) pulse sequence was employed to acquire both T_2 relaxation and quantitative data, where all acquisition parameters were held constant with exception of the 90° and 180° pulse lengths and the recycle delay times. The time between successive 180° pulses was set at 345 μs for all nuclei. Nutation curves were collected for ^{1}H, ^{19}F, and ^{31}P nuclei to determine the 90° and 180° pulse lengths. The CPMG echo trains used for quantitation were collected using 8192 echoes and 64 acquisition points for an acquisition time of 0.32 ms for each echo. The decay of the signal intensity of the echo train was fit using an exponential curve shown by equation (7),

$$y = y_0 + A_0 exp\left(-x/t\right), \quad (7)$$

where the pre-exponential factor, A_o, was used for quantitation by applying the receptivity factor, D_{cf} or D_{cB}, to determine the elemental ratios. The effect of polarity/ionicity of the sample on Q was measured as a function of frequency at magnetic fields of 0.47, 1.17, 1.88, 2.58, and 3.29 T which correspond to frequencies of approximately 20,

50, 80, 110, and 140 MHz, respectively. Q was measured using a Copper Mountain TR1300/1 vector network analyzer and was calculated by dividing the resonant frequency by the bandwidth (-6 dB).[19] Additionally, Q was also measured for frequencies ranging from 17 to 140 MHz for BTFEMP and TPP to generate a trend line for the relationship of $M_z \approx A\omega^{1.5}Q^{0.5}$, frequency, and signal intensity. Nutation curves for ^{1}H and ^{31}P were collected for each sample at all frequencies, and T_1 relaxation times were measured using the conventional inversion recovery experiment so that a 90° pulse was applied for excitation and $5*T_1$ was used for the recycle delay to acquire quantitatively comparable results. These measurements were carried out for frequencies ranging from 17 to 140 MHz for both ^{1}H and ^{31}P nuclei.

RESULTS AND DISCUSSION The CPMG experiment yields an echo train where the amplitude of the echo exponentially decays with time constant T_2^*. The decay of the signal intensity is the time that it takes for the spins in the transverse plane to lose coherence, designated as the T_2 relaxation time, and can be a result of molecular diffusion, chemical shift anisotropy, and dipolar coupling. Figure 1 shows the decay of the ^{1}H, ^{19}F, and ^{31}P signals for BTFEMP at 1 T along with an exponential fit for each curve. The signal intensity for ^{31}P is considerably smaller than the signal intensity for ^{1}H and ^{19}F due to the lower concentration and gyromagnetic ratio of the phosphorous. Consequently, the ^{31}P decay curve was multiplied by a factor of 25 to accentuate the exponential nature of the curve. The pre-exponential factor, A_0, in Equation (7) is a measure of the signal intensity and depends on the concentration of a particular isotope in solution. The T_2^* relaxation time measured in this study is representative of all environments in the sample and does not account for separate ^{1}H molecular environments. This is due to (1) low magnetic fields that do not allow for separation of chemical shift information, (2) magnetic field inhomogeneity that causes signals to be broad, and (3) the time domain analysis of the data. By fitting the decay of the signal, both parameters can be simultaneously determined, and such an analysis can be expedited by using a Matlab or Python code to generate and tabulate this information within seconds. All exponential fits were calculated with a single decay constant, which appeared to be independent of the number of ^{1}H, ^{31}P, or ^{19}F nuclei in the molecule, which is likely an artifact of the lack of resolution at the magnetic field strengths employed. In this case, the T_2^* of all environments of isotope k are combined together to give a single value rather than separating into the T_2^* for each particular environment. The T_2^* values have been measured and are reported in Table 1. For ^{1}H, ^{19}F, and ^{31}P measurements, the data shows that T_2^* decreases with increasing frequency. This is explained by the variable magnetic field strength that is applied for measurements at different frequencies. It has been noted previously that the field homogeneity of B_0 decreases as B_0 increases, and a reduction in field homogeneity has a direct influence on the T_2^* relaxation rate.[20] Since higher frequencies were achieved by increasing the strength of B_0, it can be expected that T_2^* values decrease with frequency.

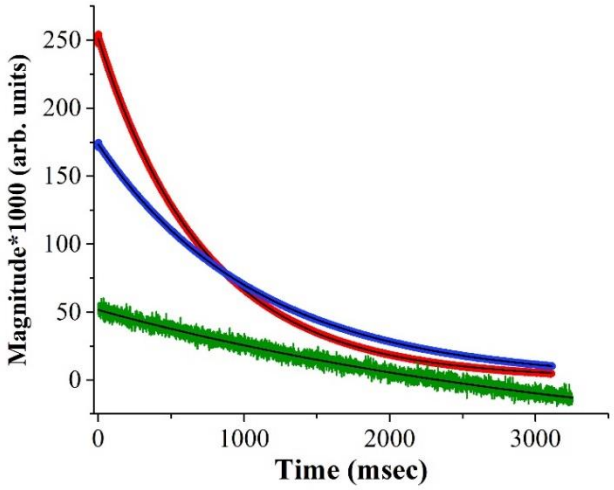

FIGURE 1. Exponential decay of the magnitude signal intensity of neat BTFEMP collected using CPMG for ^{1}H (blue), ^{19}F (red) and ^{31}P (green). The decay of the signal in the echo train is simulated using an exponential curve (black lines). The fits provide T_2^* relaxation times, as well as the pre-exponential factor that is used for quantitative measurements. Note: the ^{31}P intensity was multiplied by 25 for clarity.

Fitting the decay curves results in values for A_0 for each isotope, which is used to determine the elemental ratios. The values of A_0 are inherently tied to the concentration as well as the receptivity (γ) of the nucleus, but the receptivity effects may be corrected by using the receptivity for constant field, D_{cB}, as shown in Equation (2). Consequently, the H:F:P elemental ratios were calculated using A_0 from a CPMG echo train at 1 and 3.5 T and were corrected using D_{cB}, as shown in Table 1. The theoretical H:F:P ratio for BTFEMP is 7:6:1, and the calculated elemental ratios have been normalized to the theoretical number of hydrogen atoms. For both fields, the H:F ratios have low errors of less than 3% and are due mostly to statistical instrumental variance. All spectra were acquired in triplicates, and variance between subsequent spectra showed errors of roughly 1 %. Due to the similarity in γ for ^{1}H and ^{19}F (42.6 and 40.1 MHz/T,

TABLE 1. Elemental ratios determined using A_O from the signal decay of the echo train in CPMG experiments for BTFEMP. Gyromagnetic ratios, γ, for ^{1}H, ^{19}F, and ^{31}P are 42.58, 40.05, and 17.24 MHz/T. The theoretical H:F:P ratios for BTFEMP is 7:6:1 and experimental elemental ratios have been normalized relative to the theoretical hydrogen value. Note that A_o values have been normalized by D_{cB} and D_{cF}.

Field/Frequency	Isotope	A_o	Elemental Ratio	Error (%)	T_2^* (s)
Constant Field: B = 1T	**^{1}H**	2.50×10^5	7.00	-	0.758
	^{19}F	1.73×10^5	5.84	2.74	1.100
	^{31}P	2.80×10^3	1.18	18.20	4.009
Constant Field: B = 3.5T	**^{1}H**	1.14×10^5	7.00	-	0.932
	^{19}F	8.29×10^4	6.10	1.65	1.311
	^{31}P	1.43×10^3	1.32	32.22	3.535
Constant Frequency: ω = 42.6 MHz	**^{1}H**	2.50×10^5	7.00	-	0.758
	^{19}F	2.00×10^5	5.93	1.03	1.105
	^{31}P	1.38×10^4	0.95	4.77	3.889

respectively), the signal response is assumed to be similar and produces lower errors in the H:F ratios, as shown in Table 1. The H:P ratio, on the other hand, is higher than expected and has an error of 18.2 and 32.2% for the ratios collected at 1 and 3.5T, respectively, even after taking the constant field receptivity, D_{cB}, into consideration. In this case, D_{cB}, which only corrects for differences in γ, is not sufficient to account for the different frequencies used in a constant field experiment. The error is exaggerated at higher magnetic field (32.2% at 3.5 T compared to 18.2% at 1 T) and is attributed to the response of the probe at the different frequencies of the two nuclei, where $\Delta\omega$ is 88.7 and 25.4 MHz, respectively. According to Equation (3), the difference in frequency between ^{1}H and ^{31}P has an effect on Q, and the dependence of Q on frequency is shown in Figure 2 for BTFEMP, as well as other solutions, which will be discussed in detail below. This plot clearly illustrates that Q increases with frequency for most solutions, therefore the probe efficiency and output signal increases with frequency as well.

In order to eliminate the differences in probe efficiency, H:F:P ratios were also evaluated using the constant frequency method, and results are shown in Table 1. These results confirm the relationship of greater frequency difference with greater relative error. The frequency was held constant at 42.6 MHz and the magnetic field was swept from 1.0 to 2.5 T to collect spectra for ^{1}H, ^{19}F, and ^{31}P. Using this method, Q does not have to be taken into account, and only γ is responsible for any differences in receptivity for these measurements. Thus, signal may be corrected using D_{cf} to determine the elemental ratios. The observed H:F:P ratios for constant frequency measurements are 7:5.77:1.22, which yield errors of 1.03 and 4.77 % for fluorine and phosphorous. While the error for the H:F ratio is not affected, it was significantly reduced for the H:P ratio and can be considered as experimental error. Because the frequency was held constant, the Q factor was the same for all three nuclei, and therefore any error in these experiments is likely due to statistical instrumental variance, data processing, or the inferior signal:noise ratio (S/N) of the ^{31}P measurements.

To determine how to correct Q, ^{1}H and ^{31}P single-pulse NMR spectra where collected for neat BTFEMP and 1M TPP in deuterated DMSO at frequencies ranging from 17 to 140 MHz. The relation in Equation (5) was used to describe the dependence of frequency and Q ($\omega^{1.5}Q^{0.5}$) with signal, therefore Q was measured for all frequencies, and this is plotted in Figure 3. The results of the $\omega^{1.5}Q^{0.5}$ versus signal data are shown in a double logarithmic plot in Figure 2, and the data has been fit using a linear regression. Figure 3 shows data from both ^{1}H and ^{31}P measurements for several solutions, and the average of the slopes of the linear fit for all data sets is 1.025 ± 0.006. The low variance in the slope values signifies that for different isotopes and samples with varying Q, the rate of the increasing signal intensity with frequency remains unchanged. It further suggests that the signal intensity can be corrected for differences in frequency between nuclei for samples of various compositions and polarities. Finally, this Figure proves that the relation given in Equation 5 is valid over the range of frequencies investigated here. This is exemplified with ^{1}H and ^{31}P data that

was collected for BTFEMP at a constant magnetic field of 1.17 T with frequencies of 50.0 and 20.26 MHz, respectively. First, the ^{31}P signal intensity, acquired at 20.26 MHz, was corrected so that it is analogous to the expected ^{31}P signal intensity of BTFEMP at 50 MHz. The slope of the magnetization (M_z) versus $\omega^{1.5}Q^{0.5}$ fit, which is defined as $m = (y_2 - y_1)/(x_2 - x_1)$, is used to relate the frequency and Q difference to the acquired and expected signal intensities, as shown in Equation (8):

$$ln\left(M_{z,50.0\ MHz}\right) = e\{ln\left(M_{z,20.3\ MHz}\right) + m[ln(\omega^{1.5}Q^{0.5})_{50.0\ MHz} - ln(\omega^{1.5}Q^{0.5})_{20.3\ MHz}]\}. \quad (8)$$

Since Q was measured previously as a function of frequency, the $\ln(\omega^{1.5}Q^{0.5})$ for both frequency points can be applied to Equation (8) along with the acquired signal intensity. This leaves only the expected signal intensity at 50 MHz, which has been corrected for ω and Q.

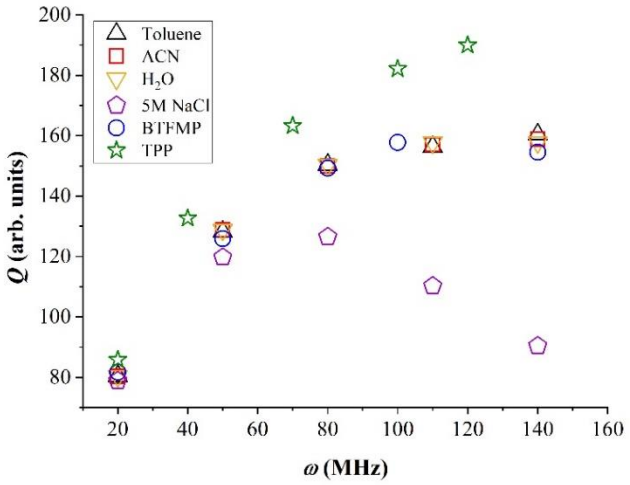

FIGURE 2. Dependence of Q on frequency, at frequencies ranging from 20 to 140 MHz for 5M NaCl (purple pentagon), water (orange inverted triangle), acetonitrile (red square), toluene (black triangle), BTFMP (blue circle), and TPP (green star) samples. The Q increases exponentially for toluene, acetonitrile, and water, but Q for 5M NaCl decreases at higher frequencies.

Now, the comparison of the ^{1}H and ^{31}P signal can be considered as a pseudo-constant frequency experiment, and D_{cf} can be used. Here, the differences in γ for ^{1}H and ^{31}P can be accounted for so that the signal intensities can be compared. Applying the correction for ω and Q and the receptivity for γ to the ^{31}P data for BTFEMP gives a H:P ratio of 7:0.95 (theoretical ratio is 7:1) with an error of 5.88%. Previously, when only the D_{cB} was applied to the data collected under constant field conditions at 1 T, the error was 18.20 %. This is significantly reduced by correcting for the probe efficiency. The Q correction has been applied to DIMP and TPP as well and both show errors of less than 6%, as is tabulated in Table 2. While determination of the probe efficiency was carried out using single pulse experiments, the two-step correction for Q can also be applied to CPMG results, where the A_o is used in place of the signal intensity. It should be noted here that this relationship is valid for only a given system, which includes the console and probe, but if either of these components is changed, then the slope of the efficiency correction factor must be reevaluated.

The above correction is described for the case where a variable field magnet is used. However, since a majority of NMR labs house static magnets, the correction should also be considered for this configuration. In order to test the viability of this method under static field conditions, ^{1}H and ^{31}P NMR spectra were collected at a field of 1.17 T (ω_H = 50 MHz and ω_P = 20.26 MHz) using a CPMG pulse sequence. A_o was measured, then divided by D_{cf}. Takeda has shown that Dcf should be used for measurements at constant frequency only since it corrects for γ. However, it is used here for constant field experiments because the signal first needs to be corrected for γ before it can be corrected for ω and Q. After applying D_{cf}, a double logarithmic plot similar to Figure 3 can be generated. This yields a plot where the data points can be fit with a line of slope 1.096. In comparison, the slope of the line fit with the variable field data was 1.005, proving that this correction can be carried out under constant field conditions as well.

TABLE 2. Elemental ratios of BTFEMP, DIMP, and TPP using Q efficiency correction factor, with elemental H:P ratios with error of less than or equal to ~6%. All data was processed using time domain signal intensities for single pulse experiments, unless otherwise stated.

Sample	Theoretical H:P	Calculated H:P	Error (%)
BTFEMP (CPMG)	7:1	7:0.96	3.6
BTFEMP	7:1	7:0.94	5.88
DIMP	17:1	17:0.94	6.05
TPP	15:1	15:1.02	2.52

^{1}H single-pulse NMR spectra were also collected and analyzed for toluene, acetonitrile, water, and 5M NaCl to determine the effect of polarity on the Q dependence of signal intensity and the results are plotted in Figures 2 and 3. The relative polarities for toluene, acetonitrile, water, and DMSO are 0.1, 0.5, 1.0, and 0.421 and this set of

solvents delineates how the slope is effected by polarity. The average slope for the linear fit of the ^{1}H and ^{31}P data for all six solutions are 1.025 ± 0.006, as shown in Figure 3, demonstrating that polarity has no effect on the relationship between the signal intensity and $\omega^{1.5}Q^{0.5}$, and therefore this relationship stays constant for other nuclei and solutions of differing polarity. This relationship also holds up for the ionic solution of 5M NaCl, even though ionic solutions tend to be problematic in NMR due to the lossiness of the sample.[21–23] The effect of polar and ionic samples has been reported previously, and is a result of dielectric and resistive losses, caused by the interaction of RF electric fields with the sample, which lowers Q and the SNR.[22] By examining the dependence of Q on frequency, the NaCl solution shows a much different behavior than other solvents, as shown in Figure 2. This is a consequence of the resistive losses typical of ionic solutions. Toluene, acetonitrile, and water all show a similar exponential growth of Q with frequency, while 5M NaCl increase to a maximum Q at 80 MHz and then decreases with higher frequencies. Although 5M NaCl has a much different behavior of Q with respect to frequency, the slope of the linear fit for $\omega^{1.5}Q^{0.5}$ is the same as for the other samples (Figure 3). As Q decreases at higher frequencies for 5M NaCl, the signal also decreases by a proportional amount, thus keeping the trend constant, and characterizing the relationship between frequency, Q, and signal.

The effect of polarity and ionicity is an issue when dealing with calibrations using external standards to build a calibration curve due to the aforementioned resistive losses. ^{19}F calibration curves, constructed using TFA in acetonitrile and deuterated water, are plotted in Figure 4. The resulting slopes of the two calibration curves are drastically different and stemm from the use of the two different solvents, acetonitrile and deuterated water, which have polarities of 0.46 and 1.11, respectively. The deuterated water, a higher polarity solvent, leads to more losses due to the higher effective resistance of the sample. The relationship of the SNR to the resistance is:

$$SNR \propto \frac{1}{\sqrt{R_s(T_s+T_{pa})+R_c(T_c+T_{pa})}}, \quad (9)$$

where R_s and R_c are the resistance values of the sample and coil, respectively, and T_s, T_{pa}, and T_c are the temperatures of the sample, preamplifier, and coil, respectively.[11] For the system used in this study, it was found that noise is constant and therefore Equation (9) can be directly related to signal intensity and the differences in signal response can be directly related to the effective resistance of the samples. For the analysis of the TFA standards in different solvents, the only term that differs is R_s, and the higher effective resistance of water over acetonitrile is expected due to polarity differences. The effect of the resistive losses is seen in the relative intensity of the two calibration curves, where the signal intensity of the deuterated water curve is lower than that of the acetonitrile for similar fluorine concentrations. The slope of the curve is also lower for the former because the sample becomes more lossy as the concentration of the TFA increases, which has previously been seen in other polar or ionic solutions.[22] According to Equation (3), the effective resistance of the sample is inversely proportional to Q, so highly polar or ionic samples should exhibit a lower Q value.

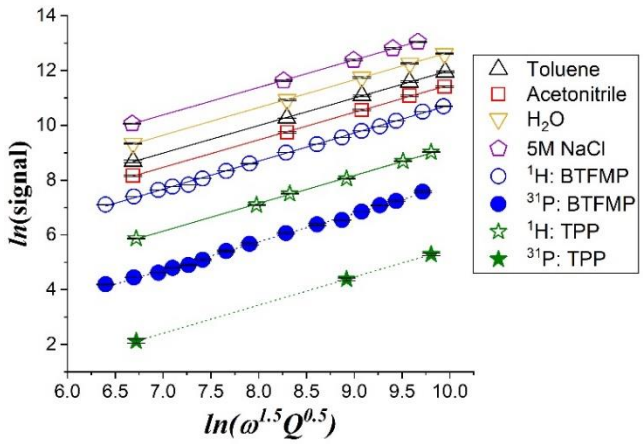

FIGURE 3. Double logarithmic plot of the signal as a function of $\omega^{1.5}Q^{0.5}$ for various solvents. Data points for ^{1}H (open symbols) and ^{31}P (solid symbols) are shown for TPP (green star), BTFEMP (blue circle), 5M NaCl (purple pentagon), water (orange inverted triangle), acetonitrile (red square), and toluene (black upright triangle). The regression line of best fit for each data set is also plotted, and all lines have a slope of 1.025 ± 0.006.

This suggests that the use of external calibration standards is not a viable method to determine elemental ratios of unknown samples where the polarity is not previously identified. For rapid analyses, the more robust process is to apply the efficiency correction that not only considers difference in γ but also corrects for the effects of Q. This approach can be widely used for ionic, organic polar and non-polar samples to identify the elemental ratios of various samples and can be especially useful in biological specimens, since water and salt contents in such samples can vary widely. While this method may be used for measurement of elemental ratios, it should be noted

here that this does not identify the absolute concentration of a particular nucleus as would be determined by using an internal or external calibration standard. However, the detection of elemental ratios for individual samples or substances does have advantages especially in the case of chemical warfare agents or concentrated pharmaceuticals which tend to have a specific number of P and/or F atoms for a certain number of H atoms and therefore elemental ratios are sufficient in these instances. By implementing CPMG to determine the elemental ratios, T_2^* values can be simultaneously measured to add another dimension to the signature space for identification of unknown samples.

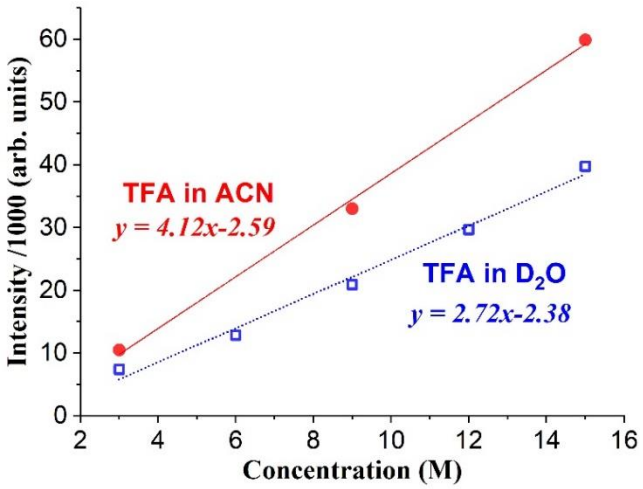

FIGURE 4. Calibration curves collected using ^{19}F NMR of trifluoro-acetic acid in either acetonitrile (red) or D_2O (blue). The calibration curves show significantly different slopes and the intensity/isotope changes drastically at higher concentrations, which is due to differences in the polarity of the two solvents. All ^{19}F NMR spectra were collected at a magnetic field of 1 T and a frequency of 40.05 MHz.

This method can be applied to NMR spectrometer systems that utilize either static or variable magnetic fields. In both cases, the circuit needs to be characterized by generating a $\ln(\omega^{1.5}Q^{0.5})$ versus ln(signal) plot, as shown in Figure 3. The following procedure describes the steps that are required for either static or variable field systems to enable rapid detection of elemental ratios without using internal or external standards.

Variable magnetic field case:

1. Using a sample, the magnetic field should be swept so that spectra can be collected for a given nucleus at different frequencies. The spectra must be collected using a $\pi/2$ pulse and a recycle delay of $5*T_1$, therefore the T_1 and a nutation curve must be generated at each frequency.

2. The Q at each frequency should needs to be recorded.

3. A plot similar to that shown in Figure 3 is generated to determine the signal response over a range of frequencies by carrying out a linear regression. This only needs to be carried out on one nucleus since the response is constant regardless of nucleus or polarity of the sample.

4. The linear regression is used to generate the line of best fit. Takeda's correction (D_{cf}) is then used to divide the signal intensity. The slope of the best fit line will be applied to Equation (8) to determine elemental ratios for other samples. There is no need to re-characterize the probe for future use.

Constant magnetic field case:

1. A single sample should also be used in the case of a constant field system. Here, since the field cannot be swept, different frequencies should be probed by acquiring spectra on each different nuclei. For example, ^{13}C and ^{29}Si could be measured on a tetramethyl silane or ^{13}C and ^{31}P on a methyl phosphate. These spectra need to be collected using a $\pi/2$ pulse and a recycle delay of $5*T_1$. It should be noted that this only works for a single channel, such as the broadband channel. The H/F channel would need to be characterized independently by collecting ^{1}H and ^{19}F spectra.

2. Q is recorded at each frequency.

3. The signal intensity, A_0, is then measured for each spectrum and normalized to make the nuclear ratios 1:1. For example, the ^{13}C signal intensity in $Si(CH_3)_4$ needs to be divided by 4. The normalized signal is then divided by D_{cf} to correct for γ.

4. A double logarithmic plot, similar to Figure 3, is constructed using the signal divided by for γ for each nucleus and then plotting against $\omega^{1.5}Q^{0.5}$.

5. Step 4 from the variable magnetic field procedure is followed to determine the elemental ratios.

CONCLUSION The ability to measure elemental ratios without the use of internal or external standards has been discussed here as a method

for rapid detection of unknown solutions, especially at low magnetic fields (1 and 3.5 T). Because the polarity of the solvent has an effect on the signal output due to dielectric losses, the implementation of calibration curves using external calibration standards is not a robust method for rapid detection. NMR signal intensities were collected using CPMG time domain analysis then corrected for (1) the Q of the probe at different frequencies and (2) the γ of each nucleus. The application of such a correction yielded elemental ratios with a 6% or less error for various material solutions. The relationship of $\omega^{1.5}Q^{0.5}$ and the signal intensity is constant for a variety of samples that have polarities ranging from 0.1 to 1.0 and even holds constant for ionic solutions. This allows the 2-step correction factor to be applied broadly for many different types of samples and eliminates the need for internal or external calibration standards if elemental ratios are satisfactory for the analysis of the unknown sample. The correction also works on static magnetic field systems, as described above. The T_2^* is simultaneously measured when the CPMG pulse sequence is employed, and therefore this analytical method allows an additional signature to be simultaneously measured to identify unknown or potentially dangerous chemicals rapidly and accurately.

AUTHOR INFORMATION

Corresponding Author

* Email: scarlettw@lanl.gov

ACKNOWLEDGMENT

The authors gratefully acknowledge R. Michalczyk, M.W. Malone, P. Magnelind, and A.V. Urbaitis for intellectual support and informative conversations in support for this study. This project was supported by the Department of Homeland Security (DHS) Science & Technology Directorate (S&T) through Interagency Agreement HSHQPM-16-X-00213 with Los Alamos National Laboratories. This work is released for publication in accordance with Los Alamos National Laboratory LA-UR-19-26783 by Triad National Security, LLC (Los Alamos, NM, USA) operator of the Los Alamos National Laboratory under Contract No. 89233218CNA000001 with the U.S. Department of Energy.

REFERENCES

(1) Mathias, A. The Detection and Estimation of the Relative Amounts of Primary and Secondary Hydroxyl Groups Using NMR. *Anal. Chim. Acta* **1964**, 31 (6), 598–601.

(2) Harris, R. K. Applications of Solid-State NMR to Pharmaceutical Polymorphism and Related Matters *. *J. Pharm. Pharmacol.* **2007**, 59, 225–239. https://doi.org/10.1211/jpp.59.2.0009.

(3) Rosen, B. R.; Belliveau, J. W.; Vevea, J. M.; Brady, J. Perfusion Imaging with NMR Contrast Agents. *Magn. Reson. Med.* **1990**, 14, 249–265.

(4) Stanley, P. D. *Organofluorines*, 1st ed.; Neilson, A. H., Ed.; Springer: New York, 2002.

(5) Flores-parra, A.; Gutierrez-avella, D. M.; Contreras, R.; Khuong-Huu, F. ^{13}C and ^{1}H NMR Investigations of Quinic Acid Derivatives : Complete Spectral Assignment and Elucidation of Preferred Conformations. *Magn. Reson. Chem.* 1989, 27, 544–555.

(6) Verpoorte, R.; Choi, T. H.; Kim, H. K. NMR-Based Metabolomics at Work in Phytochemistry. *Phytochem. Rev.* **2007**, 6, 3–14. https://doi.org/10.1007/s11101-006-9031-3.

(7) Diakos, C. I.; Messerle, B. A.; Murdoch, P. S.; Parkinson, J. A.; Sadler, P. J.; Fenton, R. R.; Hambley, T. W. Identification by NMR Spectroscopy of the Two Stereoisomers of the Platinum Complex [PtCl 2 (S -Ahaz)] (S -Ahaz) 3 (S) - Aminohexahydroazepine) Bound to a DNA 14-Mer Oligonucleotide . NMR Evidence of Structural Alteration of a Platinated A · T-Rich. *Inorg. Chem.* **2009**, 48 (7), 3047–3056.

(8) Akoka, S.; Barantin, L.; Trierweiler, M. Concentration Measurement by Proton NMR Using the ERETIC Method. *Anal. Chem.* **1999**, 71 (95), 2554–2557.

(9) Takeda, K.; Ichijo, N.; Noda, Y.; Takegoshi, K. Elemental Analysis by NMR. *J. Magn. Reson.* **2012**, 224, 48–52. https://doi.org/10.1016/j.jmr.2012.09.004.

(10) Abragam, A. *Principles of Nuclear Magnetism*; Oxford University Press: Oxford, 1961.

(11) Hoult, D. I.; Richards, R. E. The Signal-to-Noise Ratio of the Nuclear Magnetic Resonance Experiment. *J. Magn. Reson.* **1976**, 24, 71–85.

(12) Hill, H. D. .; Richards, R. E. Limits of Measurement in Magnetic Resonance. *J. Phys. E.* **1968**, 1, 977–983.

(13) Levitt, M. H. *Spin Dynamics Basics of Nuclear Magnetic Resonance*; John Wiley & Sons, Ltd: West Sussex, 2008; pp 543–595.

(14) Meiboom, S.; Gill, D. Modified Spin-Echo Method for Measuring Nuclear Relaxation Times. *Rev. Sci. Instrum.* **1958**, 29 (8), 688–691. https://doi.org/10.1063/1.1716296.

(15) Carr, H. Y.; Purcell, E. M. Effects of Diffusion on Free Precession in Nuclear Magnetic Resonance Experiments. *Phys. Rev.* **1954**, 94 (3), 630–638. https://doi.org/10.1103/PhysRev.94.630.

(16) Skidmore, K.; Hewitt, D.; Kao, Y. H. Quantitation and Characterization of Process Impuri-

ties and Extractables in Protein-Containing Solutions Using Proton NMR as a General Tool. *Biotechnol. Prog.* **2012**, 28 (6), 1526–1533. https://doi.org/10.1002/btpr.1620.

(17) Bharti, S. K.; Sinha, N.; Joshi, B. S.; Mandal, S. K.; Roy, R.; Khetrapal, C. L. Improved Quantification from ^{1}H-NMR Spectra Using Reduced Repetition Times. *Metabolomics* **2008**, 4, 367–376. https://doi.org/10.1007/s11306-008-0130-6.

(18) Van, Q. N.; Chmurny, G. N.; Veenstra, T. D. The Depletion of Protein Signals in Metabonomics Analysis with the WET-CPMG Pulse Sequence. *Biochem. Biophys. Res. Commun.* **2003**, 301 (4), 952–959. https://doi.org/10.1016/S0006-291X(03)00079-2.

(19) Doty, F. D. Probe Design and Construction. In Encyclopedia of Magnetic Resonance; 2007; pp 1–19.
https://doi.org/10.1002/9780470034590.emrstm1000.

(20) Podol'skii, A. Design Procedure for Permanent Magnet Assemblies with Uniform Magnetic Fields for MRI Devices. *IEEE Trans. Magn.* **2000**, 36 (2), 484–490. https://doi.org/10.1109/20.825819.

(21) Gadian, D. G.; Robinson, F. N. H. Radiofrequency Losses in NMR Experiments on Electrically Conducting Samples. *J. Magn. Reson.* **1979**, 34, 449–455.

(22) Robosky, L. C.; Reily, M. D.; Avizonis, D. Improving NMR Sensitivity by Use of Salt-Tolerant Cryogenically Cooled Probes. *Anal. Bioanal. Chem.* **2007**, 387, 529–532. https://doi.org/10.1007/s00216-006-0982-4.

(23) Swiet, T. M. De. Optimal Electric Fields for Different Sample Shapes in High Resolution NMR Spectroscopy. *J. Magn. Reson.* **2005**, 174, 331–334. https://doi.org/10.1016/j.jmr.2005.02.007.

Insert Table of Contents artwork here